arXiv:cond-mat/9710088v1 [cond-mat.mtrl-sci] 9 Oct 1997

Dynamic Local Distortions in Ferroelectrics

Henry Krakauer, Rici Yu,* and Cheng-Zhang Wang
Department of Physics, College of William and Mary
Williamsburg, Virginia 23187–8795

Karin M. Rabe and Umesh V. Waghmare**
Yale University, Department of Applied Physics, P. O. Box 208284
New Haven, Connecticut, 06520-8284
(October 9, 1997)

Molecular-dynamics simulations of $KNbO_3$ reveal preformed dynamic chain-like structures, present even in the paraelectric phase, that are related to the softening of phonon branches over large regions of the Brillouin zone. The phase sequence of ferroelectric transitions is correctly reproduced, showing that the first-principles effective Hamiltonian used in the simulations captures the essential behavior of the microscopic fluctuations driving the transitions. Real space chains provide a framework for understanding both the displacive and order-disorder characteristics of these phase transitions.

Submitted to Physical Review Letters

PACS: 77.80.Bh, 77.22.Ej 77.80.-e,

There are many experimental indications in perovskite ferroelectrics that the actual atomic structure in some of the phases may be significantly different locally than is indicated by the average crystallographic structure deduced from elastic X-ray and neutron scattering. Among the earliest of these, diffuse X-ray scattering measurements of Comes *et al.*, [1,2] on $KNbO_3$ and $BaTiO_3$ revealed temperature-dependent streak patterns, which were interpreted as evidence for randomly ordered static chains (oriented along [100] directions) of distorted primitive cells, even in the paraelectric cubic phase. Other observations such as quasi-elastic central peaks in neutron scattering [3] and Raman spectroscopy [4] above the phase transition temperature are also indicative of preformed clusters of the low temperature phase. More recently, pair distribution functions obtained from neutron scattering measurements up to very high momentum transfers [5] and XAFS measurements [6] indicate the presence of short-range order. First-principles calculations provide a powerful tool for probing the structural energetics of local distortions. For $KNbO_3$, LAPW linear response calculation of the zero-temperature phonon dispersion in the cubic perovskite structure reveals its instability against the formation of localized chain distortions. [7] In this paper, we explore the implications of these results for dynamical behavior at nonzero temperature through the molecular dynamics (MD) simulation of an effective Hamiltonian constructed from first-principles calculations, establishing the presence and dynamic nature of localized chain distortions above T_c.

While first-principles calculations have provided a great deal of information, they are limited to zero temperature and to relatively small simulation cells. The use of effective Hamiltonians, H_{eff}, to extend the reach of the first-principles results has proved to be a useful strategy for the quantitative analysis of temperature-driven structural phase transitions in real materials. [8,9,10] These Hamiltonians act in the subspace of the full ionic configuration space which contains the degrees of freedom relevant to the transition(s). These include, in particular, the "soft mode," identified as the unstable mode of the high-symmetry structure which freezes in to produce the low-symmetry phase(s). The coefficients in a Taylor expansion around the high-symmetry structure of the Born-Oppenheimer surface in this subspace are determined from first-principles total-energy and linear-response results. Nonzero temperature simulations using H_{eff} quantitatively reproduce the structural transition properties of the full system.

We constructed H_{eff} for $KNbO_3$ using the lattice-Wannier-function (LWF) method. [9] Full details of the construction are presented elsewhere, [11] and we give only a brief description here. The effective Hamiltonian subspace is defined using a basis of localized and symmetrized atomic displacement patterns, called lattice Wannier functions, which are constructed to reproduce the first-principles unstable polar Γ_{15} phonon as well as unstable transverse optic phonon eigenvectors and frequencies at other high-symmetry points in the BZ [7]. For $KNbO_3$, the subspace is spanned by one vector degree of freedom per unit cell, $\xi_{i\alpha}$, representing the LWF coordinates, where i = unit cell index and $\alpha = x, y, z$. We include as additional degrees of freedom the homogeneous strain tensor, which describes changes in the overall volume and shape of the simulation cell.

In the LWF basis, the kinetic energy retains a simple diagonal form. The potential energy is expressed as a Taylor expansion in the LWF coordinates $\xi_{i\alpha}$ and can be

organized as follows:

$$U = U_{on-site} + U_{short-range} + U_{dipolar} + U_{LWF-strain} + U_{elastic}. \quad (1)$$

We include anharmonic terms only in the on-site interaction $U_{on-site} = \kappa\xi_i^2 + \delta\xi_i^4 + \gamma(\xi_{ix}^2\xi_{iy}^2 + c.p.)$, and in the lowest order coupling between LWF coordinates (on-site quadratic) and homogeneous strain (linear) $U_{LWF-strain}$. Strain coupling of this type has been shown to be crucial in obtaining the experimentally observed sequence of ferroelectric phase transitions in perovskite ferroelectrics. [8,12] The coefficients of the on-site anharmonic and strain coupling terms were determined by fitting to first-principles total energies, varying strain and amplitude of uniform LWF distortions in the [100], [110] and [111] directions. The interactions between LWF coordinates in different unit cells are included to quadratic order only, with the general form $\sum_{ij\alpha\beta} J_{ij\alpha\beta}\xi_{i\alpha}\xi_{j\beta}$. Beyond third neighbor, the $J_{ij\alpha\beta}$ are parameterized as the interaction between two dipoles $Z^*\vec{\xi}_i$ and $Z^*\vec{\xi}_j$, where Z^* is the mode effective charge for the unstable zone-center phonon, screened by the electronic dielectric constant ε_∞. Z^* and ε_∞ are computed directly using LAPW linear response, while the short-range $J_{ij\alpha\beta}$ are fit to the first-principles dynamical-matrix elements.

Using H_{eff}, classical molecular dynamics simulations were carried out for a $10 \times 10 \times 10$ simulation cell, corresponding to 5000 atoms, with periodic boundary conditions; the $\xi_{i\alpha}$'s in H_{eff} are in units of $10a$, where $a = 4.016\mathring{A}$ is the lattice constant. A variable cell shape formalism was used together with Nosé-Hoover thermostats to equilibrate the MD runs at constant temperature. [13] After equilibration, and prior to computing the static and dynamic structure factors, the thermostats were turned off and the cell shape and volume were kept fixed. Further equilibration (constant-energy MD) generally caused the temperature to change by about 5 K. After this last equilibration, MD runs of typically 20000 time steps (each time step $\sim$ 1 femtosecond) were performed. The static and dynamic structure factors and autocorrelation functions of the $\xi_{i\alpha}$'s were then computed [14] using data from every 10th time step.

The different structural phases and transition temperatures T_c are identified in the MD simulations by calculating the three components of the order-parameter S_α, defined as an average over the LWF coordinates: $S_\alpha = (1/N)\sum_i \xi_{i\alpha}$. For example, the time average of all three components of the order parameter is zero at 400 K in $KNbO_3$, indicating that the system is in the cubic paraelectric phase. At 370 K, one of the components of the order parameter freezes out with a non-zero average value of about 0.16, but the time average of the other two components is still zero, indicating that the system is in the tetragonal phase. Subsequent freezing out of the other components signals transitions to the orthorhombic and rhombohedral phases. The MD T_c values were calculated by us for $KNbO_3$ and, as a calibration of the method, for $BaTiO_3$, using the H_{eff} constructed in Ref. [8]. The results, given in Table I, are an average of cooling and heating runs, and we estimate the error in these numbers to be about 5 - 10 K.

TABLE I. Comparison of calculated and measured transition temperatures (see text), between the rhombohedral (R), orthorhombic (O), tetragonal (T) and cubic (C) phases. Temperatures are in Kelvin.

	R - O	O - T	T - C
$KNbO_3$			
MD	210	260	370
Exper.[c]	210 - 265	488	701
$BaTiO_3$			
MD	200	230	290
MC[a]	197	230	290
Exper.[b]	183	278	403

[a]Ref. [8].
[b]From Ref. [8].
[c]See for example, M. D. Fontana, G. Metrat, J. L. Servoin and F. Gervais, *J. Phys. C* **16**, 483 (1984).

The calculated T_c for the cubic-tetragonal transition is significantly underestimated in both materials, and the error is considerably larger in $KNbO_3$ than in $BaTiO_3$ and $PbTiO_3$ [10]. T_c's for the R-O and O-T are in better agreement, with the R-O agreement being the best. Possible sources of this quantitative discrepancy include the use of the local density approximation, the neglect of higher-order coupling to degrees of freedom outside the effective Hamiltonian subspace, and the sensitivity of the transition to residual inaccuracies in the parametrization of strain coupling. In any case, the nontrivial phase sequence and the trend from $BaTiO_3$ to $KNbO_3$ are correctly reproduced, suggesting that the effective Hamiltonian captures the essential behavior of the microscopic fluctuations driving the transitions.

Turning to the soft-mode vibrational frequencies, the temperature dependence of the soft-mode dispersion in $KNbO_3$ is shown in Fig. 1 and compared with the 798 K cubic phase inelastic neutron scattering measurement of Holma and Chen. [15] The dispersion and temperature dependence were determined from the dispersion of pronounced peaks in the Fourier transformed autocorrelation function obtained from the MD simulations. The experimental data is taken about 100 K above the cubic-tetragonal phase transition. The 400 K MD results are 30 K above the calculated transition temperature. The agreement is good below $q \sim 0.2$, with the theoretical TO branch showing greater dispersion for larger q. This branch was unusually difficult to measure for $q \geq 0$, [15] however, the measured peak intensity being extremely low and the background unusually high.

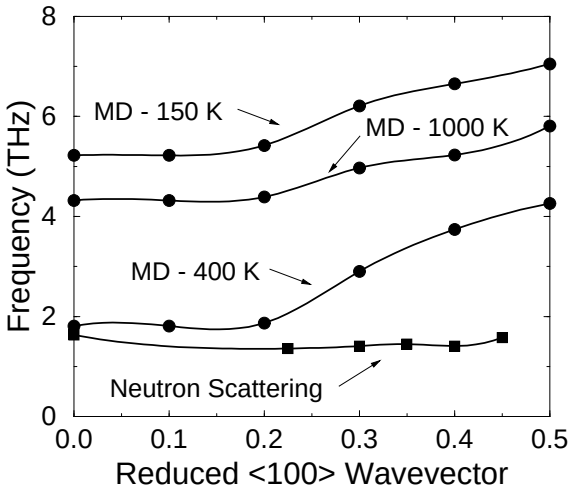


FIG. 1. Comparison of the soft-mode dispersion along the [100] direction. Neutron scattering data from Ref. [15] in the cubic phase of $KNbO_3$ at 798 K. In the MD simulations, the system is in the cubic phase at 400 and 1000 K and in the rhombohedral phase at 150 K.

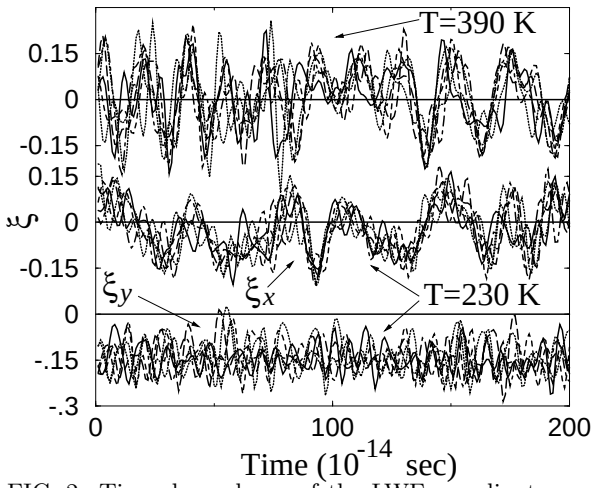


FIG. 2. Time dependence of the LWF coordinate components ξ_{ix} and ξ_{iy} in the orthorhombic (230 K) and cubic (390 K) phases of $KNbO_3$, for six ($i = 0...5$) adjacent primitive cells along an uncondensed chain in the x-direction (see text). R_y and R_z are condensed but $R_x = 0$. Chain-like correlations are evident in the correlated motion of the six LWF coordinates ξ_{ix} as a function of time, but not in the y components, which oscillate randomly about the condensed value of -0.16.

The most striking feature in Fig. 1 is that the *entire* TO branch softens by about 2 THz on cooling from 1000 K to 400 K. This behavior differs from the usual soft-mode picture of a displacive phase transition, in which softening occurs only in the vicinity of the wavevector associated with the structural phase transition. It is consistent, however, with the previously obtained first-principles LAPW linear response results. [7] These revealed regions of instability in the BZ described by three mutually perpendicular interpenetrating slabs centered at Γ, perpendicular to the cubic axes, and extending to the BZ boundaries. The first-principles unstable TO mode is seen in Ref. [7] to also disperse slightly upwards in frequency from Γ to the X point, consistent with what is found here. In the MD simulations, however, the harmonically unstable first-principles TO branch is anharmonically stabilized.

The fact that an entire phonon branch softens, *i.e.* the softening occurs simultaneously over large regions of the BZ, suggests that the analysis should focus on the temperature dependence of the structure in real space rather than in reciprocal space. Tending more to a order-disorder picture, this also would naturally incorporate the interpretation of the experimental observations of local atomic structure, such as the streak patterns observed in diffuse X-ray scattering in $BaTiO_3$ and $KNbO_3$. [2] Comes *et al.* invoked scattering from disordered finite-length static chains of distorted primitive cells to explain this behavior, proposing an empirical model in which there is sequential ordering of chains directed along the three cubic axes. Thus, for example, in the cubic to tetragonal transition, the ordering of the z-axis chains corresponds to the disappearence of the incoherent scattering (circular streaks in Fig. 6a of Ref. [2]) due to randomly oriented z-chains. Subsequent ordering of the x-axis and y-axis chains corresponds to entering the orthorhombic and rhombohedral phases, with all the chains being ordered in the ground state rhombohedral phase. The *ab initio* linear response calculations of Yu and Krakauer [7] on $KNbO_3$ provided theoretical support for the empirical chain model of Comes *et al.* by showing the existence of BZ planar instabilities. Furthermore, simulated diffuse elastic X-ray scattering intensities calculated from MD simulations on $BaTiO_3$ reproduce the observed position and sequential disappearance of the three families (circles, vertical and horizontal) of streak patterns on cooling from the cubic to rhombohedral phases. [16]

Diffuse X-ray scattering cannot, however, distinguish between static and dynamic chains. Using MD simulations, we can resolve this issue. Fig. 2 shows the time dependence of the LWF coordinates in the orthorhombic (230 K) and cubic (390 K) phases of $KNbO_3$, for six adjacent primitive cells along the x-direction. In the cubic phase all three order parameters are zero. In the orthorhombic phase the order parameters S_y and S_z are condensed, but the average value of S_x is zero, corresponding to disordered uncondensed chains along the x-direction. Chain-like correlations are evident in the correlated motion of the longitudinal LWF components as a function of time in this figure. (Due to the use of periodic boundary conditions in the $10 \times 10 \times 10$ simulation

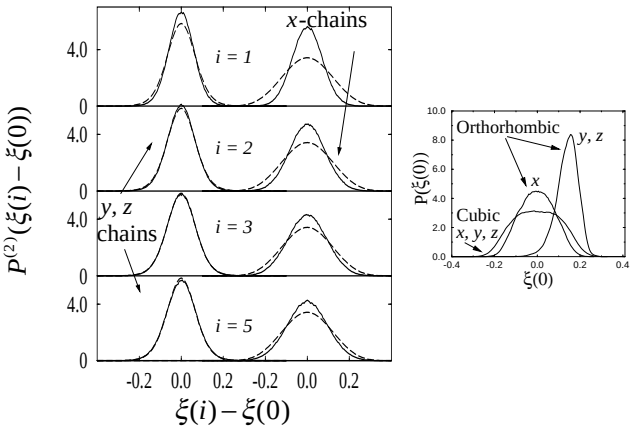


FIG. 3. The solid lines are two-site equal-time probability distributions, $P^{(2)}(\xi(i) - \xi(0))$, for i=1,2,3, and 5 along condensed y and z chains and for uncondensed x chains in orthorhombic $KNbO_3$. In both cases, ξ represents the longitudinal component of the LWF coordinate along the chain direction. The dashed lines are obtained using the one-site probability distribution, assuming no correlation between the two sites. The inset shows the one site probability distributions, $P(\xi(0))$, for the x, y, and z components in the orthorhombic phase, as well as in the cubic phase.

cell, the largest nearest neighbor distance along a chain is $5a$.) As expected from the linear response calculations [7], the y- and z-components of the atoms in an x-chain should be uncorrelated, and this is confirmed in Fig. 2. Similarly if we examine the longitudinal (or transverse) LWF components along condensed y- or z-chains (not shown) there is no correlation. Chain correlation is still evident even as high as 1000 K in the cubic phase, but the characteristic chain reversal frequency increases as a function of temperature. Fig. 3 gives a more quantitative account of the correlated motions.

These results unambiguously show 1) the existence in real space of chains and 2) the *dynamic* character of the chains. This agrees with the conclusions of Holma *et al.* [17], based on their diffuse X-ray measurements, and with the empirical lattice dynamics model of Hüller [18]. The MD simulations show that the chains are preformed well above the cubic-tetragonal phase transition temperature. The chains are defined by rows of distorted primitive cells oriented along the three cubic axes, with the atomic displacements along the chain highly correlated with one other. Displacements in different chains are uncorrelated at high temperature, and the observed phase transitions correspond to the sequential freezing or onset of coherence of families of chains along the three cubic axes. The softening of entire branches of unstable TO modes gives rise to these real space chains and provides a framework for understanding both the displacive and order-disorder characteristics of these phase transitions.

ACKNOWLEDGMENTS

Work at William and Mary was supported by Office of Naval Research grant N00014-97-0049. Work at Yale was supported by ONR grant N00014-97-1-0047 and the Alfred P. Sloan Foundation. Computations were carried out at the Cornell Theory Center. We are also pleased to acknowledge the assistance of J. Broughton with the molecular dynamics algorithms.

* Present address: General Sciences Corporation, Laurel, MD 20707.
** Present address: Dept. of Physics, Harvard Univ., Cambridge, MA 02138.

[1] R. Comes, M. Lambert and A. Guinier, *Sol. State Commun.* **6**, 715 (1968).
[2] R. Comes, M. Lambert and A. Guinier, *Acta Cryst.* **A26**, 244 (1970).
[3] S. M. Shapiro, J. D. Axe and G. Shirane, *Phys. Rev.* **B 6**, 4332 (1972).
[4] M. D. Fontana, H. Idrissi, G. E. Kugel and K. Wojcik, *J. Phys. Condens. Matter* **3**, 8695 (1991).
[5] S. Teslic, T. Egami and D. Viehland, *J. Physics and Chem. Solids* **57**, 1537 (1996).
[6] E. A. Stern and Y. Yacoby, *J. Physics and Chem. Solids* **57**, 1449 (1996).
[7] R. Yu and H. Krakauer, *Phys. Rev. Lett.* **74**, 4067 (1995).
[8] W. Zhong, D. Vanderbilt, and K. M. Rabe, *Phys. Rev. Lett.* **73**, 1861 (1994).
[9] K. M. Rabe and U. V. Waghmare, *Phys. Rev. B* **52**, 13236 (1995).
[10] U. V. Waghmare and K. M. Rabe, *Phys. Rev. B* **55**, 6161 (1997).
[11] H. Krakauer, R. Yu, C.-Z. Wang, and U. V. Waghmare, and K. M. Rabe, unpublished.
[12] K. M. Rabe and U. V. Waghmare, *Ferroelectrics* **194**, 118 (1997).
[13] J. V. Lill and J. Broughton, *Phys. Rev. B* **46**, 12068 (1992); J. Broughton, private communication.
[14] T. Schneider and E. Stoll, *Phys. Rev. B* **17**, 1302 (1978).
[15] M. Holma and H. Chen, *J. Phys. Chem. Solids* **57**, 1465 (1996). We have reversed the assignment of the transverse acoustic and transverse optic branches near the zone boundary as given in this reference. H. Chen has confirmed this correction, private communication.
[16] H. Krakauer, R. Yu, C.-Z. Wang, and C. LaSota, *Ferroelectrics*, in press.
[17] M. Holma, N. Takesue and H. Chen, *Ferroelectrics* **164**, 237 (1995).
[18] A. Hüller, *Solid State Commun.* **7**, 589 (1969); *ibid. Z. Physik.* **220**, 145 (1969).